Spin-state Regulation of Iron(III) Centres by Axial Ligands with Tetradentate Bis(picolinamide) In-plane Ligands†

Manabendra Ray,[a] Rabindranath Mukherjee,*[,a] John F. Richardson[b] and Robert M. Buchanan[b]

[a] *Department of Chemistry, Indian Institute of Technology, Kanpur 208 016, India*

[b] *Department of Chemistry, University of Louisville, Louisville, KY, 40292, USA*

Mononuclear iron(III) complexes *trans*-$[Fe(bpb)X_2]^{+/-}$ [H_2bpb = 1,2-bis(pyridine-2-carboxamido)-benzene; X = pyridine (py) **1**, N_3^- **2**, $MeCO_2^-$ **3** or CN^- **4**] and *trans*-$[Fe(bpc)X_2]^{+/-}$ [H_2bpc = 4,5-dichloro-1,2-bis(pyridine-2-carboxamido)benzene; X = py **5**, Cl^- **6** or $MeCO_2^-$ **7**] have been synthesised and characterized. Complexes **1** and **4** are low-spin (μ_{eff} = 2.50 and 2.10 at 298 K, solution phase) whereas **2**, **3**, **6** and **7** (μ_{eff} = 5.86–5.98 at 298 K, solution phase) are high spin. Solid-state magnetic susceptibility (40–300 K) and Mössbauer spectral measurements at 300 and 77 K of **1** and **7** confirmed the spin state. The complex $[NEt_4][Fe(bpc)(MeCO_2)_2]\cdot CHCl_3$ **7** has been characterized by X-ray crystallography: space group $P2_1/c$, a = 12.283(3), b = 18.819(3), c = 16.437(3) Å, β = 101.02(2)°, Z = 4, R = R' = 0.041 for 5069 observed reflections. The solid-state EPR spectra (300 and 77 K) of **1**, **4** and **5** are typical of low-spin iron(III) and have been analysed to determine the ligand-field parameters. All the complexes display ligand-to-metal charge-transfer transitions in the visible region (550–800 nm). Cyclic voltammetric measurements of **1** in pyridine and **4** in dimethylformamide revealed a quasi-reversible Fe^{III}–Fe^{II} reduction [$E_{\frac{1}{2}}$ = −0.06 V, ΔE_p = 150 mV for **1** and $E_{\frac{1}{2}}$ = −0.83 V, ΔE_p = 100 mV for **4** *vs.* saturated calomel electrode (SCE)]. The high-spin complexes exhibit an electrochemically irreversible but chemically reversible Fe^{III}–Fe^{II} reduction (E_{pc} = −0.44 to −0.83 V) in acetonitrile solution. Complexes **2**, **4** and **6** show a reversible one-electron oxidation ($E_{\frac{1}{2}}$ = +0.66 to +1.05 V *vs.* SCE).

Control of the spin state by axial ligands in porphyrinatoiron derivatives has been recognized as an important factor in the structure–function relationships of haemoproteins.[1] A change in spin state has also been observed[2] in the non-haem antibiotic bleomycin–iron(III) complex[2] having a characteristic Fe–N-(amide) bond.

Within the class of six-co-ordinate complexes *trans*-$[Fe^{III}LX_2]$, with L = a neutral or a dinegative tetradentate N_4 ligand (excluding porphyrins and phthalocyanins) and X = a neutral or an uninegative monodentate axial ligand, only a very limited number of molecules have been described as high or low spin.[3,4] When L is dinegative three complexes are known and all are low spin.[4] To date no complex of this class with a dinegative open-chain tetradentate N_4 ligand system has been reported to reveal a change in spin state upon variation of the axial ligands.

As part of our continued interest[5] in the transition-metal chemistry of dianionic bis(picolinamide) in-plane ligands herein we describe the syntheses and magnetic and spectroscopic characterization of a group of diaxially ligated complexes with bpb(2−) [H_2bpb = 1,2-bis(pyridine-2-carboxamido)benzene] and bpc(2−) [H_2bpc = 4,5-dichloro-1,2-bis(pyridine-2-carboxamido)benzene]. The axial ligands include pyridine (py), Cl^-, N_3^-, $MeCO_2^-$ or CN^-. Our primary concern is to demonstrate how the spin state of an iron(III) centre can be tuned in its complexes by merely changing the axial ligands. The crystal structure of a representative complex $[NEt_4][trans\text{-}Fe^{III}(bpc)(MeCO_2)_2]\cdot CHCl_3$ has been determined. The cyclic voltammetric behaviour of these complexes has also been investigated. Since the completion of this work, two independent reports of iron(III) complexes using the present ligand system have appeared;[6] however, neither demonstrated the spin-state variation of the iron(III) centre with a given in-plane ligand.

† *Supplementary data available:* see Instructions for Authors, *J. Chem. Soc., Dalton Trans.*, 1993, Issue 1, pp. xxiii–xxviii.

Experimental

Chemicals and Starting Materials.—Solvents and reagents were obtained from commercial sources and used without further purification unless otherwise stated. Acetonitrile, dimethylformamide (dmf), diethyl ether, chloroform and pyridine were purified as before.[5a,7] The reagents 1,2-diamino-4,5-dichlorobenzene, triphenyl phosphite and tetraethylammonium acetate tetrahydrate were from Aldrich Chemical Co. The complexes $[Fe(MeCN)_4][ClO_4]_2$[8] and $[NEt_4][FeCl_4]$[9] and the ligands H_2bpb[10] and H_2bpc[11] were prepared following the literature methods.

Syntheses of Metal Complexes.—All the complexes were synthesised for the first time. **CAUTION**: perchlorate salts should be handled with care.

$[Fe(bpb)(py)_2]ClO_4$ **1**. A solution of $[Fe(MeCN)_4][ClO_4]_2$ (1.33 g, 3.18 mmol) in MeCN (10 cm^3) was slowly added to a solution containing H_2bpb (1.00 g, 3.16 mmol) and pyridine (1.01 cm^3, 12.55 mmol) in MeCN (20 cm^3). The resulting deep reddish brown solution was stirred for 1 h and cooled in a refrigerator. The reddish brown crystalline precipitate formed was filtered off, washed with MeCN (1 cm^3) and dried *in vacuo* (yield *ca.* 80%) (Found: C, 53.70; H, 3.65; N, 13.15. Calc. for $C_{28}H_{22}ClFeN_6O_6$: C, 53.40; H, 3.50; N, 13.35%). IR: ν(amide I) 1630 and ν(ClO_4) 1100 cm^{-1}. Λ_M = 120 Ω^{-1} cm^2 mol^{-1} in MeCN, μ_{eff} in pyridine 2.50. Variable-temperature magnetic moment (T/K, μ_{eff}): 300, 2.44; 275, 2.39; 250, 2.37; 225, 2.35; 200, 2.32; 180, 2.30; 160, 2.29; 140, 2.30; 120, 2.25; 100, 2.24; 81, 2.23; 62, 2.22; 52, 2.23; 42, 2.21. Mössbauer (δ/mm s^{-1}, ΔE_Q/mm s^{-1}): 0.12, 2.36 at 300 K and 0.18, 2.36 at 77 K.

$[NEt_4][Fe(bpb)(N_3)_2]$ **2**. Solid H_2bpb (0.16 g, 0.5 mmol) was added portionwise with stirring to a solution of $[Fe(MeCN)_4][ClO_4]_2$ (0.21 g, 0.5 mmol) in MeCN (10 cm^3). The resulting orange-brown solution was stirred for 5 min and a solution of $[NEt_4][N_3]$ (0.18 g, 1.04 mmol) in methanol (2 cm^3) was added. The solution immediately turned dark greenish brown and was stirred for 5 min and NEt_3 diluted 1:10 in MeCN (1.4 cm^3, 0.5 mmol) was added. The resulting deep green solution was stirred for 5 min and the solvent removed under vacuum. The solid was redissolved in MeCN (5 cm^3) and filtered. Diethyl ether (5 cm^3) was added to the filtrate and kept in a freezer. The complex was isolated as deep green crystals and dried *in vacuo* (yield 37%) (Found: C, 53.40; H, 6.00; N, 26.20. Calc. for $C_{26}H_{32}FeN_{11}O_2$: C, 53.25; H, 5.50; N, 26.25%). IR: $\nu(N_3)$ 2020, ν(amide I) 1600 cm^{-1}. Λ_M = 120 Ω^{-1} cm^2 mol^{-1} in MeCN, μ_{eff} in MeCN 5.98. Powder EPR: 5.278, 2.127 at 300 K.

$[NEt_4][Fe(bpb)(MeCO_2)_2]\cdot H_2O$ **3**. The complex $[Fe(bpb)(py)_2]ClO_4$ (0.52 g, 0.83 mmol) was stirred in MeCN (5 cm^3). To this stirred solution was added dropwise $[NEt_4][MeCO_2]\cdot 4H_2O$ (0.45 g, 1.72 mmol) in MeCN (1 cm^3). The solution immediately turned deep green and was stirred for 1 h, filtered and concentrated to *ca.* 3 cm^3. Diethyl ether (1.5 cm^3) was added and the solution kept in a refrigerator. After 24 h the green crystals formed were filtered off, washed with acetonitrile–diethyl ether (1:2, *ca.* 2 cm^3), and dried *in vacuo* (yield *ca.* 50%) (Found: C, 56.60; H, 5.90; N, 10.70. Calc. for $C_{30}H_{40}FeN_5O_7$: C, 56.45; H, 6.30; N, 10.95%). IR: ν(amide I) and ν(acetate) 1610 and 1620 cm^{-1}. Λ_M = 120 Ω^{-1} cm^2 mol^{-1} in MeCN, μ_{eff} in MeCN 5.86. Powder EPR: 7.900 (br), 4.770 (br), 2.850 at 300 K.

Alternatively, $[NEt_4][Fe(bpb)(py)_2]$ (0.10 g, 0.17 mmol) was stirred with an excess of $[NEt_4][MeCO_2]\cdot 4H_2O$ (0.10 g, 0.37 mmol) in MeCN for 24 h. Addition of diethyl ether to the concentrated solution yields green crystals (yield *ca.* 80%).

$Na[Fe(bpb)(CN)_2]$ **4**. The complex $[Fe(bpb)(py)_2]ClO_4$ (0.11 g, 0.18 mmol) and NaCN (0.10 g, 2.04 mmol) were stirred in ethanol (10 cm^3) for 2 h. The reddish brown suspension immediately dissolved generating a deep green solution and dark green crystals started to separate within 15 min. The product and excess of NaCN were filtered off and washed with ethanol. The solid was redissolved in dmf, filtered to remove the excess of NaCN and solvent evaporated under reduced pressure. The residue was dissolved in ethanol (5 cm^3) and diethyl ether (5 cm^3) added. The solution afforded dark green (almost black) crystals after cooling for 1 d. The product was filtered off and dried *in vacuo* (yield *ca.* 75%) (Found: C, 53.90; H, 3.00; N, 18.60. Calc. for $C_{20}H_{12}FeN_6NaO_2$: C, 53.70; H, 2.70; N, 18.80%). IR: ν(amide I) 1620 and $\nu(C\equiv N)$ 2140 cm^{-1}. Λ_M = 70 Ω^{-1} cm^2 mol^{-1} in dmf, μ_{eff} in dmf 2.10.

$[Fe(bpc)(py)_2]ClO_4$ **5**. A mixture of H_2bpc (0.193 g, 0.5 mmol) and $[Fe(MeCN)_4][ClO_4]_2$ (0.220 g, 0.52 mmol) in acetonitrile (20 cm^3) was stirred at 60 °C for 5 min. To the resulting yellow solution pyridine (0.2 cm^3, 2 mmol) was added and stirred for 5 min. The deep red solution thus formed was filtered immediately and cooled in a freezer. The product that formed before filtration was contaminated with H_2bpc and thus rejected. The deep red crystals isolated from the filtrate were dried *in vacuo* (yield 40%) (Found: C, 48.40; H, 3.00; N, 11.90. Calc. for $C_{28}H_{20}Cl_3FeN_6O_6$: C, 48.15; H, 2.90; N, 12.05%). IR: ν(amide I) 1620 and $\nu(ClO_4)$ 1100 and 620 cm^{-1}. Solid-state magnetic moment μ_{eff} 2.18.

$[NEt_4][Fe(bpc)Cl_2]$ **6**. A solution of $[NEt_4][FeCl_4]$ (0.20 g, 0.61 mmol) in dmf (10 cm^3) was stirred for 2 min and then solid H_2bpc (0.24 g, 0.62 mmol) was added with stirring. The suspension thus obtained was stirred for 10 min and NEt_3 diluted 1:10 in dmf (1.7 cm^3, 1.23 mmol) was added dropwise. The mixture immediately turned deep green. It was warmed on a water-bath for 5 min, stirred for 2 h and then filtered. The resulting solution was evaporated to dryness and MeCN (5 cm^3) added. On cooling the product separated as dark green crystals, which were filtered off and recrystallized from acetonitrile–diethyl ether (10 cm^3) (yield *ca.* 43%). This complex is fairly stable in the air (Found: C, 48.85; H, 5.10; N, 10.80. Calc. for $C_{26}H_{30}Cl_4FeN_5O_2$: C, 48.60; H, 4.70; N, 10.90%). IR: ν(amide I) 1620 cm^{-1}. Λ_M = 120 Ω^{-1} cm^2 mol^{-1} in MeCN. μ_{eff}: in MeCN, 5.90; solid state, 5.96. Powder EPR: 4.28w at 300 K.

$[NEt_4][Fe(bpc)(MeCO_2)_2]\cdot CHCl_3$ **7**. A solution of $[Fe(MeCN)_4][ClO_4]_2$ (0.11 g, 0.27 mmol) in dmf (2 cm^3) was added dropwise to a solution containing H_2bpc (0.10 g, 0.26 mmol) and $[NEt_4][MeCO_2]\cdot 4H_2O$ (0.28 g, 1.08 mmol) in dmf (5 cm^3). The solution immediately turned dark brown and was stirred for 1 h. The solvent was removed under vacuum and to the residue MeCN (5 cm^3) was added. The resulting greenish violet solution gave a violet powder on addition of diethyl ether (10 cm^3), which was recrystallized from chloroform–hexane to afford reddish violet crystals (yield *ca.* 55%) (Found: C, 46.50; H, 5.00; N, 8.90. Calc. for $C_{31}H_{37}Cl_5FeN_5O_6$: C, 46.05; H, 4.60; N, 8.65%). IR: ν(acetate) and ν(amide I) 1600 and 1620 (sh) cm^{-1}. Λ_M = 120 Ω^{-1} cm^2 mol^{-1} in MeCN. Solution magnetic moment μ_{eff} 5.90 in MeCN. Variable-temperature magnetic moment (T/K, μ_{eff}): 300, 5.99; 275, 5.95; 250, 5.99; 225, 6.09; 200, 5.95; 180, 5.91; 160, 5.92; 140, 5.93; 120, 5.86; 100, 5.81; 81, 5.89; 62, 5.82; 52, 5.72; 42, 6.06. Mössbauer (δ/mm s^{-1}, ΔE_Q/mm s^{-1}): 0.35, 0.82 at 300 K and 0.45, 0.88 at 77 K. Powder EPR: 5.220 (br) and 2.020w at 300 K.

Alternatively, $[NEt_4][Fe(bpc)Cl_2]$ (0.10 g, 0.15 mmol) was stirred with an excess of $Na(O_2CMe)$ in MeCN (5 cm^3) for 24 h. The NaCl which formed was filtered off and the filtrate evaporated to dryness giving a violet powder (yield *ca.* 0.10 g, *ca.* 95%). The complex was recrystallized from chloroform–hexane. The products from both methods gave identical IR and absorption spectra.

The single crystals of complex **7** suitable for X-ray diffraction studies were grown by slow evaporation of a dilute solution of the complex in chloroform–hexane (1:4 v/v, 20 cm^3) over a period of 2 d.

Measurements.—Infrared spectra were recorded as KBr pellets on a Perkin Elmer 1320 spectrophotometer, electronic spectra on a Perkin Elmer Lambda 2 spectrophotometer. Solution electrical conductivity was measured in MeCN solutions with an Elico type CM-82 T conductivity bridge (Hyderabad, India) with solute concentrations of *ca.* 10^{-3} mol dm^{-3}. Solution magnetic susceptibility measurements were done by the conventional NMR method[12] in acetonitrile with a PMX-60 JEOL (60 MHz) spectrometer. Solvent susceptibility[13a] and diamagnetic corrections[13b] were taken from published data.

Variable-temperature magnetic susceptibility measurements were made on powdered samples over the range 40–300 K by the Faraday method as described previously.[14] Effective magnetic moments were calculated using the formula $\mu_{eff} = 2.828(\chi_M T)^{\frac{1}{2}}$, where χ_M is the corrected molar susceptibility. The diamagnetic contributions were calculated by using literature tabulations.[13b] All measurements were made at a fixed field strength and the field dependence of the magnetic susceptibility was not studied.

Mössbauer spectral measurements were done as described previously[14] and with reference to metallic iron at room temperature. The observed spectra were computer-fitted by Lorentzian lines as described earlier.[14]

X-Band EPR spectra were recorded with a Varian E-109 C spectrometer fitted with a quartz Dewar for measurements at liquid-dinitrogen temperature. The spectra were calibrated with diphenylpicrylhydrazyl, dpph (g = 2.0037).

Cyclic voltammetry and coulometric measurements were performed by using a PAR model 370-4 electrochemistry system incorporating the following: model 174 A polarographic analyser; model 175 universal programmer; model 173 potentiostat/galvanostat; model 179 digital coulometer; model RE-0074 x–y recorder. Details of the measurements were as described.[5a,15]

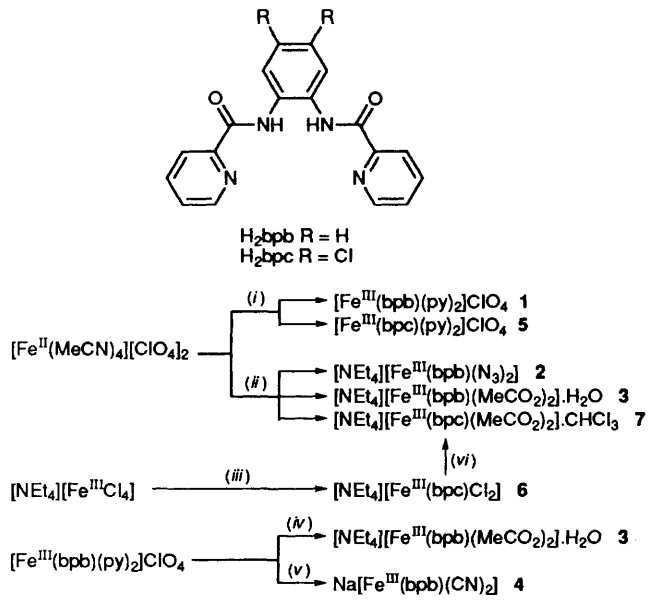

Scheme 1 *Reagents:* (*i*) H_2bpb or H_2bpc, pyridine, MeCN; (*ii*) H_2bpb or H_2bpc, $[NEt_4][N_3]$ or $[NEt_4][O_2CMe]$, dmf or MeCN; (*iii*) H_2bpc, NEt_3, dmf; (*iv*) $[NEt_4][O_2CMe]$, MeCN; (*v*) NaCN, MeCN; (*vi*) $Na(O_2CMe)$, MeCN

Crystal Structure Determination of $[NEt_4][Fe(bpc)(MeCO_2)_2]\cdot CHCl_3$.—*Crystal data.* $C_{31}H_{37}Cl_5FeN_5O_6$, M = 808.78, monoclinic, space group $P2_1/c$, a = 12.283(3), b = 18.819(3), c = 16.437(3) Å, β = 101.02(2)°, U = 3729.5 Å^3, D_m = 1.45 g cm^{-3}, Z = 4, D_c = 1.44 g cm^{-3}, $F(000)$ = 1668, λ(Mo-Kα) = 0.709 30 Å, μ = 8.1 cm^{-1}. Crystal dimensions: 0.25 × 0.35 × 0.40 mm.

Data collection and processing. A violet plate-like crystal was mounted on a glass fibre in a random orientation. Intensities (ω–2θ mode with $2\theta_{max}$ 50°, scan width = 0.8 + 0.340 tanθ, scan speed 1–3° min^{-1}, graphite-monochromated Mo-Kα radiation) were measured at 23 °C on an Enraf-Nonius CAD4 diffractometer (University of Louisville) and corrected for Lorentz and polarization effects. An empirical absorption correction was applied (correction factors 0.97–1.00). Details of the experimental technique have been described elsewhere.[16] A total of 6914 reflections were measured of which 6666 were unique, giving 5069 with $I > 3\sigma(I)$. No decay correction was applied.

Structure analysis and refinement. The structure was solved by direct methods.[17,18] Subsequent Fourier difference synthesis revealed the positions of the remaining non-hydrogen atoms. Hydrogen atoms were located and added to the structure-factor calculations but their positions were not refined. The structure was refined by a full-matrix least-squares method with anisotropic thermal parameters for the non-hydrogen atoms. The function minimized was $\Sigma w(|F_o| - |F_c|)^2$ with $w = 4F_o^2/\sigma^2(F_o^2)$. The maximum and minimum peaks on the final Fourier-difference map corresponded to 0.48 and −0.41 e Å^{-3}, respectively. All calculations were performed using the Enraf-Nonius SDP/VAX[19] package. The final weighted R factor (on F) was 0.041 and the unweighted R factor was 0.041. Atomic scattering factors, corrected for anomalous dispersion, were taken from ref. 20. The final atomic coordinates are given in Table 1.

Additional material available from the Cambridge Crystallographic Data Centre comprises H-atom coordinates, thermal parameters, and remaining bond lengths and angles.

Results and Discussion

Syntheses and Selected Properties.—The syntheses of the mononuclear diaxially ligated iron(III) complexes are outlined in Scheme 1. These reactions offer a general route to new iron(III) complexes of types $[FeL(py)_2]^+$ and $[FeLX_2]^-$ (L = bpb or bpc; X = Cl, N_3, $MeCO_2$ or CN).

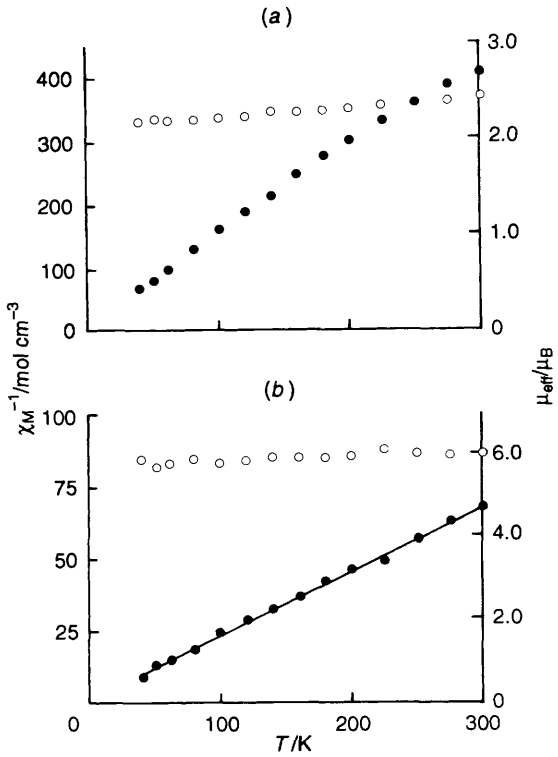

Fig. 1 Temperature dependencies of the inverse magnetic susceptibilities (●) and effective magnetic moments (○) of complexes **1** (*a*) and **7** (*b*)

In 1991 Valentine and co-workers[6a] reported the synthesis and crystal structure of $[NEt_3H][Fe(bpb)Cl_2]\cdot MeCN$; the complex was very moisture sensitive and all manipulations were therefore performed under an argon atmosphere. However, we employed a different methodology and also used substituted ligands, and the complexes obtained are sufficiently stable in the air. In 1992 Che *et al.*[6b] reported the syntheses of a series of iron(III) low-spin complexes of bpc including $[Fe(bpc)(bpy)_2]ClO_4$ (bpy = 4-*tert*-butylpyridine); however, our synthetic strategies are very different (see below).

The IR spectra of the complexes indicate that the ligands are deprotonated.[5a,b] That of **3** shows broad absorption at *ca.* 3400 cm^{-1} indicating the presence of water of crystallization. The presence of axial ligands was revealed by their characteristic vibrations. Complexes **1** and **5** show characteristic ionic perchlorate bands at 1100 and at 620 cm^{-1}. For **4**, ν(C≡N) occurs at 2140 cm^{-1} (free cyanide absorbs at 2080 cm^{-1}).[21] This shift towards higher energy upon co-ordination indicates that the cyanides act as σ-donor rather than as π-acceptor groups.[21]

Solution electrical conductivity data show that all the complexes are 1 : 1 electrolytes (Experimental section).[22] Based on the above facts and analytical data (Experimental section) we propose the formulation of the new complexes as in Scheme 1.

Magnetism and Mössbauer Spectra.—The magnetic susceptibilities of all the complexes in solution (except **5**, owing to solubility reasons) and for **1** and **5**–**7** in the solid state at ambient temperature (Experimental section) were determined. The data indicate that **1**, **4** and **5** are low spin and **2**, **3**, **6** and **7** are high spin, both in solid and solution.

In order to substantiate the spin states of these complexes, variable-temperature solid-state magnetic susceptibility studies were performed on two representative complexes **1** and **7** using the Faraday method on powdered samples in the range 40–300 K (Fig. 1). For **1** as the temperature is lowered the moment decreases towards the spin-only value as expected.[23] Never-

theless, the magnetic data show that the ground state is a spin doublet. For **7** the μ_{eff} value remained constant over the temperature range, consistent with a $^6A_1$ ground state. The Weiss constant θ and Curie constant C are calculated to be 5.576° and 4.570 cm^3 K mol^{-1} respectively. These values are in good agreement with θ values calculated for known magnetically dilute iron(III) high-spin complexes ($-7 \leqslant \theta \leqslant 5$).[24]

The spin states of complexes **1** and **7** are fully corroborated by ^{57}Fe Mössbauer spectral measurements (Fig. 2). The Mössbauer parameters (Experimental section) are symptomatic of low- and high-spin iron(III) respectively.[25]

Crystal Structure of $[NEt_4][Fe(bpc)(MeCO_2)_2]\cdot CHCl_3$ **7**.—An ORTEP[26] drawing of the anion together with the atom-labelling scheme is shown in Fig. 3. Table 2 contains selected bond distances and angles.

The iron atom sits above the mean plane of the four N atoms of the planar bpc ligand, 0.036 Å towards O(5). The axially co-ordinated acetate groups are almost perpendicular (dihedral angle between the benzene ring and the plane containing the two acetates 89.80°) to the bpc plane giving rise to a C_{2v} metal site symmetry.

The Fe–N(amide) distance in the high-spin complex $[NEt_3H][Fe^{III}(bpb)Cl_2]\cdot MeCN$[6a] is 0.03 Å shorter than that of **7**. This small increase in bond distance in **7** indicates the weaker co-ordinating ability of bpc compared to bpb due to the presence of two chloro substituents in the benzene ring. The *ca.* 0.02 Å longer Fe–N(py) bond in **7** compared to that in $[NEt_3H][Fe(bpb)Cl_2]\cdot MeCN$[6a] also supports the weaker co-ordinating ability of bpc. However, the Fe–N(amide) bond distance of the six-co-ordinate low-spin iron(III) complex $[Fe(bpc)(mim)_2]ClO_4$ (mim = 1-methylimidazole)[6b] is significantly shorter (0.178 Å) than that of the present complex. This is possibly due to the smaller size of the iron(III) centre in the former complex.

The average Fe–N(py) bond distance in the present complex is 2.205 Å, whereas that in the high-spin iron(III) complex $[H_5O_2][Fe(pydca)_2]$ (pydca = pyridine-2,6-dicarboxylate) varies between 2.0037 and 2.0076 Å.[27] This large difference arises from the increased strain exerted by the bpc ligand. This is also evident in the case of the N(py)–Fe–N(py) angle, which deviates from 90° (perfect octahedron) to 131.02° in the present case. The present ligand geometry is such that the pyridine nitrogens are unable to come closer to the metal centre, hence the observed longer Fe–N(py) bond as well as the large deviation in N(py)–Fe–N(py) angle. This type of deviation is also present in copper, rhodium and cobalt complexes with the related bpb ligand.[28]

The average axial Fe–O(acetate) bond length is 0.20 Å shorter than the Fe–Cl bond of $[NEt_3H][Fe(bpb)Cl_2]\cdot MeCN$.[6a] The axial Fe–O(acetate) bonds in high-spin $[Fe(Hedta)(H_2O)]$[29] (Hedta = monoprotonated ethane-1,2-diamine-*N*,*N*,*N*′,*N*′-tetraacetate) vary between 1.954 and 2.006 Å and are comparable to the average Fe–O(acetate) of 1.965 Å in **7**. The shorter axial bond length in the present complex indicates the greater influence of the axial acetate ligands than that of the in-plane donor atoms. This may be one of the factors which causes longer in-plane bond lengths. The behaviour of the bpc ligand is similar in known structures.[6b,30]

Absorption Spectra.—All the complexes show in the solid state (Nujol mull) and in solution intense absorptions in the visible region (Table 3). Considerable shifts were observed in going from solid to solution probably due to solvent-induced structural changes. However, the spectral profile and trends within similar complexes remain unchanged in solution (see below). As these low-energy transitions are of ligand-to-metal charge-transfer (l.m.c.t.) origin (see below) they are expected to be perturbed by the solvent polarity. In addition all the complexes show very intense absorptions in the UV region possibly due to intra-ligand transitions.[5]

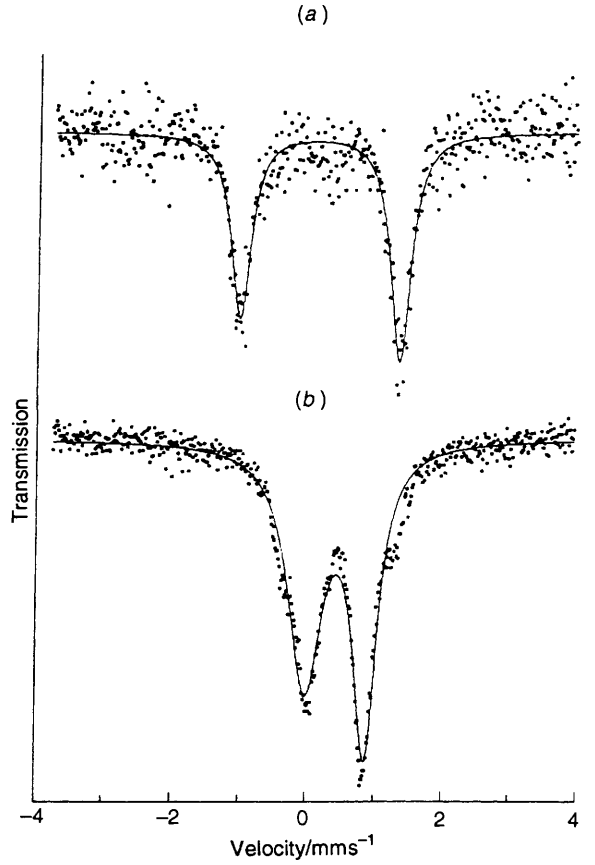

Fig. 2 Mössbauer spectra of complexes **1** (*a*) and **7** (*b*) at 77 K

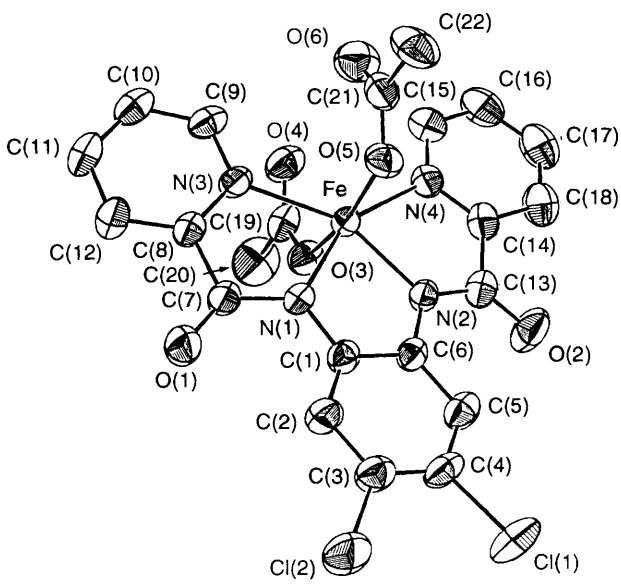

Fig. 3 The molecular structure of $[NEt_4][Fe(bpc)(MeCO_2)_2]\cdot CHCl_3$ **7** showing the atom labelling scheme

The low-energy absorptions for low-spin complexes are characteristically red shifted compared to high-spin complexes (Table 3). This could be explained as follows. For a given stereochemistry, in going from a high- to a low-spin complex the acceptor orbital will be more stabilized and as a result the l.m.c.t. transition energies are expected to shift to lower energy.

Among high-spin complexes with invariant in-plane ligands, the low-energy absorptions shift considerably to higher energy with increasing field strength of the axial ligand (Table 3). In contrast, keeping the axial ligands fixed, a change in the in-plane ligand from bpb to bpc causes a measurable blue shift. These

Table 1 Fractional atomic coordinates for non-hydrogen atoms in $[NEt_4][Fe(bpc)(MeCO_2)_2]\cdot CHCl_3$ **7** with estimated standard deviations (e.s.d.s) in parentheses

Atom	*x*	*y*	*z*	Atom	*x*	*y*	*z*
Fe	0.724 31(3)	0.215 40(2)	0.538 62(2)	C(8)	0.791 1(2)	0.065 5(2)	0.510 6(2)
Cl(1)	1.168 61(7)	0.416 24(5)	0.462 33(6)	C(9)	0.632 2(3)	0.059 2(2)	0.565 3(2)
Cl(2)	1.250 41(7)	0.255 37(6)	0.448 31(7)	C(10)	0.629 3(3)	−0.013 7(2)	0.556 8(2)
Cl(3)	0.427 7(2)	0.022 99(9)	0.713 4(1)	C(11)	0.708 7(3)	−0.047 2(2)	0.522 6(2)
Cl(4)	0.418 0(2)	0.117 5(1)	0.847 48(9)	C(12)	0.792 2(3)	−0.007 3(2)	0.499 0(2)
Cl(5)	0.314 4(2)	0.155 1(2)	0.682 8(1)	C(13)	0.748 9(3)	0.371 2(2)	0.515 5(2)
O(1)	0.956 3(2)	0.083 4(1)	0.459 7(2)	C(14)	0.640 2(3)	0.364 5(2)	0.544 4(2)
O(2)	0.778 4(2)	0.429 8(1)	0.495 0(2)	C(15)	0.508 7(3)	0.290 7(2)	0.582 3(2)
O(3)	0.635 9(2)	0.206 2(1)	0.426 1(1)	C(16)	0.444 0(3)	0.348 4(2)	0.594 6(2)
O(4)	0.478 5(2)	0.168 3(1)	0.457 9(2)	C(17)	0.480 5(3)	0.415 7(2)	0.582 8(2)
O(5)	0.780 7(2)	0.216 1(1)	0.659 7(1)	C(18)	0.580 2(3)	0.424 3(2)	0.556 4(2)
O(6)	0.626 5(2)	0.174 8(1)	0.691 8(2)	C(19)	0.534 9(3)	0.184 8(2)	0.407 4(2)
N(1)	0.869 3(2)	0.180 1(1)	0.506 7(1)	C(20)	0.488 8(4)	0.180 7(3)	0.316 1(3)
N(2)	0.802 2(2)	0.308 9(1)	0.516 7(1)	C(21)	0.722 1(3)	0.195 4(2)	0.712 0(2)
N(3)	0.712 5(2)	0.098 6(1)	0.542 7(1)	C(22)	0.777 4(3)	0.199 5(2)	0.801 8(2)
N(4)	0.606 2(2)	0.298 6(1)	0.558 2(1)	C(23)	0.912 1(4)	0.069 7(3)	0.196 5(3)
N(5)	1.031 2(3)	0.055 7(2)	0.238 7(2)	C(24)	0.836 7(4)	0.092 2(3)	0.253 7(4)
C(1)	0.945 6(2)	0.232 0(2)	0.493 4(2)	C(25)	1.038 2(4)	−0.001 4(3)	0.304 8(2)
C(2)	1.051 1(2)	0.219 1(2)	0.478 7(2)	C(26)	0.986 1(5)	−0.071 6(3)	0.274 0(3)
C(3)	1.119 7(3)	0.275 6(2)	0.467 5(2)	C(27)	1.082 1(4)	0.121 8(3)	0.283 1(3)
C(4)	1.083 4(3)	0.344 1(2)	0.471 5(2)	C(28)	1.080 4(6)	0.186 2(3)	0.227 2(4)
C(5)	0.977 9(3)	0.358 5(2)	0.486 2(2)	C(29)	1.092 0(4)	0.032 8(3)	0.170 7(2)
C(6)	0.908 1(2)	0.302 8(2)	0.498 2(2)	C(30)	1.213 4(5)	0.017 2(3)	0.198 5(3)
C(7)	0.882 1(2)	0.111 3(2)	0.489 2(2)	C(31)	0.424 4(4)	0.111 4(3)	0.744 0(3)

Table 2 Selected bond distances (Å) and angles (°) in $[NEt_4][Fe(bpc)(MeCO_2)_2]\cdot CHCl_3$ **7**

Fe–N(1)	2.061(2)	Fe–N(2)	2.067(2)
Fe–N(3)	2.205(2)	Fe–N(4)	2.199(3)
Fe–O(3)	1.965(2)	Fe–O(5)	1.979(2)
N(1)–Fe–N(2)	77.20(9)	N(2)–Fe–N(4)	76.12(9)
N(1)–Fe–N(4)	153.26(9)	N(2)–Fe–N(3)	152.8(1)
N(3)–Fe–N(4)	131.02(9)	N(3)–Fe–N(1)	75.60(9)
N(4)–Fe–O(3)	86.53(9)	N(4)–Fe–O(5)	87.82(9)
N(3)–Fe–O(3)	84.99(8)	N(3)–Fe–O(5)	89.33(9)
N(2)–Fe–O(3)	95.85(9)	N(2)–Fe–O(5)	94.91(9)
N(1)–Fe–O(3)	94.63(9)	N(1)–Fe–O(5)	96.03(9)
O(3)–Fe–O(5)	166.28(9)		

results (Table 3) point to an important generalization: the effect of a change in axial ligands is more than that of one in the in-plane ligands.

EPR Spectra.—The monomeric low-spin iron(III) complexes display characteristic rhombic *g* tensors the principal values of which are extremely sensitive to the nature of the axial ligands.[30] The EPR spectra of **1** and **5** in the polycrystalline state at 77 K show rhombic low-spin iron(III) behaviour with three principal *g* values (Table 4). Complex **4** under similar conditions shows only a broad isotropic signal at *g* *ca.* 2.13, however in dmf solution at 77 K it exhibits an axial spectrum with two principal *g* values (Table 4, Fig. 4).

We have analysed the *g* values obtained for complexes **1**, **4** and **5** according to the well established theory for the low-spin d^5 system.[30] The single solution thus obtained gives the axial (Δ/λ) and rhombic distortion parameters (V/λ). The values *a*, *b* and *c* are the orbital coefficients in the Kramers ground-state doublet wavefunction.[30b,c] In strict octahedral symmetry $a = \sqrt{2/3}$, $b = \sqrt{1/3}$, and $c = 0$. The solutions for our complexes as well as for selected reported systems are given in Table 4.

The values for complexes **1** and **4** show that the geometry deviates from a perfect octahedron. The ground state of both complexes is generally consistent with an electronic distribution $(d_{xz,yz})^4(d_{xy})^1$. Although **1** and **4** have identical in-plane ligands, the different co-ordinating ability of the axial ligands fine tunes

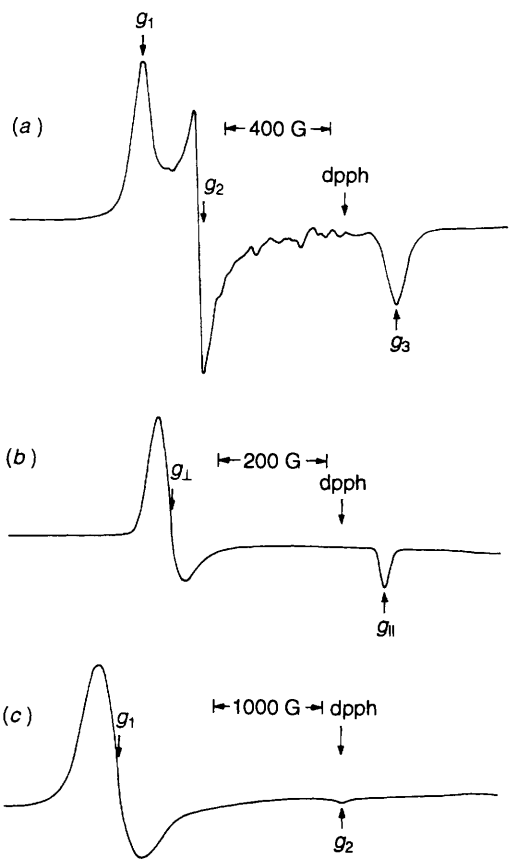

Fig. 4 Polycrystalline EPR spectra of complexes **1** (*a*) and **7** (*c*) and of a dmf glass of **4** (*b*) at 77 K; G = 10^{-4} T

the geometry in such a way that the rhombicity for cyanide complex **4** becomes zero. However, it is interesting that the rhombicity for the pyridine complex **1** is 0.29.

The powder spectra of complexes **2**, **3**, **6** and **7** show the high-spin iron(III) nature (Experimental section). It is to be noted that the crystal structures of $[NEt_3H][Fe(bpb)Cl_2]\cdot MeCN$ and **7**

Table 3 Electronic spectra[a] and cyclic voltammetric[b] data of iron(III) complexes at 298 K

			bpb/bpc oxidation		Fe^{III}–Fe^{II} couple		
Complex	Solvent	λ/nm (ε/dm³ mol⁻¹ cm⁻¹)	$E_{\frac{1}{2}}$/V	ΔE_p/mV	E_{pc}/V	E_{pa}/V	ΔE_p/mV
1	Solid[c]	915, 820 (sh),[d] 590 (sh), 450 (sh), 380, 264, 230 (sh)					
	Pyridine	780 (950), 510 (sh) (1800), 350 (sh) (9800)	—	—	−0.13	0.02	150
2	Solid	682, 497, 273					
	MeCN	633 (1300), 410 (sh) (10 700), 354 (13 200), 260 (26 600), 245 (27 000)	0.70	80	−0.54	−0.34	200
3	Solid	618, 430, 285					
	MeCN	585 (850), 345 (12 200), 265 (23 000), 221 (24 200)	0.80[e]	—	−0.83	−0.23	600
4	Solid	800, 615 (sh), 570 (sh), 475 (sh), 430, 280					
	dmf	702 (1700), 630 (sh) (1400), 579 (1300), 480 (sh) (3100), 415 (sh) (8200), 361 (10 500), 285 (sh) (11 000)	0.66	80	−0.88	−0.78	100
5[f]	Solid	901, 801 (sh), 566 (sh), 466 (sh), 420 (sh), 383, 267, 225 (sh)					
6	Solid	710, 480, 390, 300					
	MeCN	650 (1200), 350 (15 800), 300 (sh) (16 400), 270 (26 200), 230 (sh) (31 300)	1.05[g]	90	−0.44	−0.00	400
7	Solid	580 (sh), 390					
	MeCN	560 (800), 345 (14 400), 270 (25 400)	0.93[e]	—	−0.72	−0.16	560

[a] Spectral measurements in the range 500–1100 nm were made at *ca.* 10^{-3} mol dm^{-3} and for the range 200–500 nm at *ca.* 10^{-4} mol dm^{-3}. [b] Supporting electrolyte $NBu^n_4ClO_4$ (0.15 mol dm^{-3}); all potentials are referenced to the SCE; $E_{\frac{1}{2}} = 0.5(E_{pc} + E_{pa})$ where E_{pc} and E_{pa} are the cathodic and anodic peak potentials respectively; scan rate 50 mV s^{-1} at a glassy carbon electrode. [c] Solid spectra were taken in Nujol mull. [d] sh = Shoulder. [e] E_{pa} as oxidation followed by adsorption at electrode surface occurs. [f] Insoluble in pyridine (see text). [g] A second irreversible oxidation was observed at +1.4 V (E_{pa}).

Table 4 X-Band EPR data, MO coefficients and distortion parameters for the low-spin iron(III) complexes

Complex	g_x	g_y	g_z	a	b	c	Δ/λ	V/λ	V/Δ
1	2.182	2.258	1.943	0.099	0.995	−0.013	7.65	2.25	0.29
4	2.218	2.218	1.955	0.087	0.996	0.000	8.50	0.00	—
5	2.201	2.268	1.937	0.104	0.994	−0.012	7.25	1.75	0.24
$[FeL^1(MeCN)_2]^{3+}$ [a]	2.219	2.329	1.959	0.078	0.996	−0.014	9.72	3.62	0.37
$[FeL^2]^{3+}$ [a]	2.463	2.841	1.631	0.240	0.969	−0.045	3.32	1.50	0.45
$[FeL^3(mim)_2]^{+}$ [b]	1.570	2.290	2.900	0.850	0.130	−0.510	−3.40	2.07	0.61

[a] L^1 is the tetradentate N_4 bis[difluoro(dimethylglyoximato)borate] macrocycle and L^2 is a hexadentate N_6 macrocyclic ligand.[3f] [b] L^3 = Dimethyl 3,7,12,17-tetramethyl-8,13-divinylporphyrin-2,18-dipropanoate.[3f]

reveal a wide variation of the axial bond lengths and this is reflected in their EPR spectra.[6b] As the fine details of the EPR spectra of complexes depend on the nature of both axial as well as in-plane ligands, the former complex shows a typical high-spin rhombic spectrum ($g = 4.28$) and the latter shows a high-spin axial feature (Experimental section).[31] Nevertheless, the axially ligated acetate and chloride complexes show EPR spectra of essentially high-spin nature.[31]

Electrochemistry.—Electrochemical experiments were carried out primarily to reveal the effect of the axial ligands on the thermodynamic stability of the iron(III) state towards reduction.

(*a*) *Low-spin complexes*. The cyclic voltammogram of complex **1** in pyridine shows (Fig. 5) a quasi-reversible[15] reduction [$E_{\frac{1}{2}} = -0.06$ V *vs.* saturated calomel electroce (SCE), ΔE_p 150 mV] due to a Fe^{III}–Fe^{II} couple (Table 3). No other well defined redox waves were seen within the potential range +0.7 to −1.0 V. On the other hand, **4** in dmf solution exhibits a one-electron reduction (as judged by the current heights of authenticated one-electron redox responses)[5] corresponding to a Fe^{III}–Fe^{II} couple at $E_{\frac{1}{2}}$ −0.83 V *vs.* SCE ($\Delta E_p = 100$ mV); compared to the behaviour of **1** this wave is substantially cathodically shifted. This reveals that CN^- ion stabilizes the iron(III) state significantly, implying that it behaves as a strong σ-donating ligand (see above). Amongst all the axial ligands chosen in this work, it has the largest stabilizing power towards iron(III) (Table 3). Owing to the poor solubility, complex **5** could not be studied.

The cyanide complex shows an additional oxidative response at +0.66 V (Table 3, Fig. 5). The one-electron nature of this oxidation was confirmed by constant-potential electrolysis at 1.0 V.

(*b*) *High-spin complexes*. All the complexes show an electrochemically irreversible but chemically reversible Fe^{III}–Fe^{II} reduction in MeCN (Table 3) and a representative cyclic voltammogram is displayed in Fig. 5. This could be due to a change in the spin-state of the iron centre in the +II oxidation state.

These complexes show an additional quasi-reversible oxidative response (Fig. 5, Table 3). The wave is reversible to quasi-reversible in the case of Cl^- as axial ligands. However, this wave is not very well defined in the case of the $MeCO_2^-$ complexes due to interference from adsorption of the electroactive species on the electrode surface. A similar oxidative response has been found in the case of cobalt(III) complexes of the bpb and bpc ligands[5b] and believed to be ligand centred.

Conclusion

In the present investigation we have explored a rare system comprising Fe–N(amide) bonding where the spin state is regulated by the manipulation of axial ligands. The major achievements are as follows: (*i*) a series of iron(III) complexes

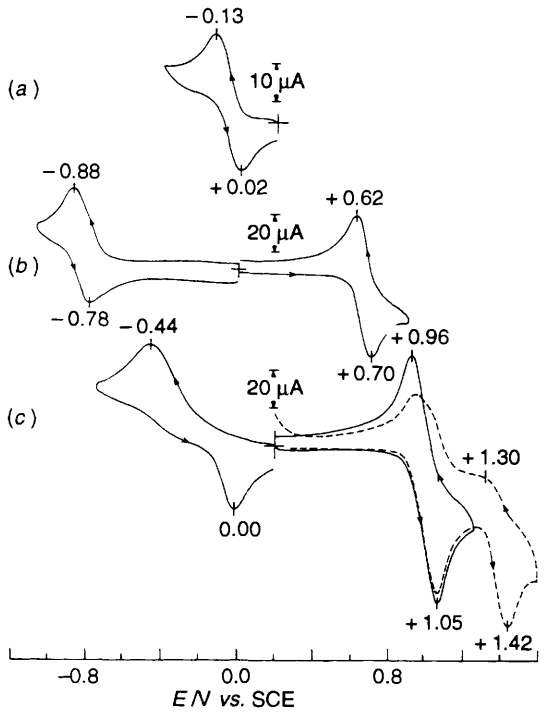

Fig. 5 Cyclic voltammograms of complexes **1** (*a*) in pyridine, **4** (*b*) in dmf and **6** (*c*) in MeCN solution at a glassy carbon electrode: scan rate 50 mV s^{-1}

have been synthesised with a deprotonated amide ligand which are indeed rare;[32] (*ii*) a versatile synthetic strategy has been developed which utilizes the lability of the axial ligands to afford a wide variety of axially substituted complexes bypassing the inherent problem of using a base with iron(III) salts; (*iii*) it has been shown possible to manipulate the spin state of the iron(III) complexes by simply changing the axial ligands, keeping the in-plane ligation fixed (this is really a very rare situation with non-porphyrin N_4 ligand systems[3,4] and appears for the first time with an open-chain ligand system) and (*iv*) the low-spin complexes display a facile Fe^{III}–Fe^{II} reduction whereas for high-spin complexes the couple is electrochemically irreversible.

Acknowledgements

We thank the Department of Science and Technology and Council of Scientific and Industrial Research, New Delhi, India, for financial assistance, Professor S. Mitra and Mr. B. T. Kansara, Chemical Physics Group and Dr. A. K. Nigam and Mr. R. S. Sannabhadti, Low-temperature Physics Group, of Tata Institute of Fundamental Research, Bombay, India for their help with variable-temperature magnetic susceptibility and Mössbauer spectral measurements respectively and Dr. T. R. Rao, Banaras Hindu University, Varanasi, India, for his help in the solid-state magnetic susceptibility measurements on some of the complexes. The comments of the referees were much appreciated.

References

1 W. R. Scheidt and C. A. Reed, *Chem. Rev.*, 1981, **81**, 543.
2 J. P. Albertini and A. Garnier-Suillerot, *Biochemistry*, 1984, **23**, 47; S. M. Hecht, *Acc. Chem. Res.*, 1989, **19**, 383.
3 (*a*) V. L. Goedken, P. H. Merrell and D. H. Busch, *J. Am. Chem. Soc.*, 1972, **94**, 3397; (*b*) D. P. Riley, P. H. Merrell, J. A. Stone and D. H. Busch, *Inorg. Chem.*, 1975, **14**, 490; (*c*) J. C. Dabrowiak and D. H. Busch, *Inorg. Chem.*, 1975, **14**, 1881; (*d*) D. W. Reichgott and N. J. Rose, *J. Am. Chem. Soc.*, 1977, **99**, 1813; (*e*) M. J. Maroney, E. O. Fey, D. A. Baldwin, R. E. Stenkamp, L. H. Jensen and N. J. Rose, *Inorg. Chem.*, 1986, **25**, 1409; (*f*) D. V. Stynes, H. Noglik and D. W. Thompson, *Inorg. Chem.*, 1991, **30**, 4567.
4 S. Koch, R. H. Holm and R. B. Frankel, *J. Am. Chem. Soc.*, 1975, **97**, 6714; P. K. Chan and C. K. Poon, *J. Chem. Soc., Dalton Trans.*, 1976, 858; Y. Nishida, S. Oshio, S. Kida and Y. Maeda, *Inorg. Chim. Acta*, 1978, **26**, 207; Y. Nishida, A. Sumita, K. Hayashida, H. Ohshima, S. Kida and Y. Maeda, *J. Coord. Chem.*, 1979, **9**, 161.
5 (*a*) M. Ray, S. Mukerjee and R. N. Mukherjee, *J. Chem. Soc., Dalton Trans.*, 1990, 3635; (*b*) M. Ray and R. N. Mukherjee, *Polyhedron*, 1992, **11**, 2929; (*c*) M. Ray and R. N. Mukherjee, unpublished work.
6 (*a*) Y. Yang, F. Diederich and J. S. Valentine, *J. Am. Chem. Soc.*, 1991, **113**, 7195; (*b*) C. M. Che, W. H. Leung, C. K. Li, H. Y. Cheng and S. M. Peng, *Inorg. Chim. Acta*, 1992, **196**, 43.
7 K. Ramesh, D. Bhuniya and R. N. Mukherjee, *J. Chem. Soc., Dalton Trans.*, 1991, 2917.
8 H. Sugimoto and D. T. Sawyer, *J. Am. Chem. Soc.*, 1985, **107**, 5712; S. A. Richert, P. K. S. Tsang and D. T. Sawyer, *Inorg. Chem.*, 1989, **28**, 2471.
9 A. P. Ginsberg and M. B. Robin, *Inorg. Chem.*, 1963, **2**, 817.
10 D. J. Barnes, R. L. Chapman, R. S. Vagg and E. C. Watton, *J. Chem. Eng. Data*, 1978, **23**, 349.
11 W. H. Leung, J. X. Ma, V. W. W. Yam, C. M. Che and C. K. Poon, *J. Chem. Soc., Dalton Trans.*, 1991, 1071.
12 D. F. Evans, *J. Chem. Soc.*, 1959, 2003.
13 (*a*) W. Gerger, U. Mayer and V. Gutmann, *Monatsch. Chem.*, 1977, **108**, 417; (*b*) C. J. O'Connor, *Prog. Inorg. Chem.*, 1982, **29**, 203.
14 S. Mahapatra, N. Gupta and R. N. Mukherjee, *J. Chem. Soc., Dalton Trans.*, 1992, 3041.
15 N. Gupta, S. Mukerjee, S. Mahapatra, M. Ray and R. N. Mukherjee, *Inorg. Chem.*, 1992, **31**, 139.
16 M. S. Mashuta, R. J. Webb, J. K. McCuster, E. A. Schmitt, K. J. Oberhausen, J. F. Richardson, R. M. Buchanan and D. N. Hendrickson, *J. Am. Chem. Soc.*, 1992, **114**, 3815.
17 C. J. Gilmore, MITHRIL, An Integrated Direct Methods Computer Program, *J. Appl. Crystallogr.*, 1984, **17**, 42.
18 P. T. Beurskens, DIRDIF, Direct Methods for Difference Structures, An Automatic Procedure Phase Extension and Refinement of Different Structure Factors, Technical Report 1984/1, Crystallography Laboratory, Toernooiveld, 1984.
19 B. A. Frenz, in *Computing in Crystallography*, eds. H. Schenk, R. Olthof-Hazelkamp, H. van Konigsveld and G. C. Bassi, Delft University Press, Delft, 1978, pp. 64–71.
20 D. T. Cromer and J. T. Waber, *International Tables for X-Ray Crystallography*, Kynoch Press, Birmingham, 1974, vol. 4, Table 2.2 B.
21 K. Nakamoto, *Infrared Spectra of Inorganic and Coordination Compounds*, 2nd edn., Wiley, New York, 1970, p. 187.
22 W. J. Geary, *Coord. Chem. Rev.*, 1971, **7**, 81.
23 L. L. Martin, R. L. Martin, K. S. Murray and A. M. Sargeson, *Inorg. Chem.*, 1990, **29**, 1387.
24 B. N. Figgis and J. Lewis, *Prog. Inorg. Chem.*, 1964, **6**, 37.
25 N. E. Erickson, *Adv. Chem.*, 1967, **68**, 86; E. A. V. Ebsworth, D. W. H. Rankin and S. Cradock, *Structural Methods in Inorganic Chemistry*, Blackwell Scientific Publications, Oxford, 1987, pp. 280–303.
26 C. K. Johnson, ORTEP II, Report ONRL-5138, Oak Ridge National Laboratory, Oak Ridge, TN, 1976.
27 J. F. Hseu, J. J. Chen, C. C. Chuang, H. H. Wei, M. C. Cheng, Y. Wang and Y. D. Yao, *Inorg. Chim. Acta*, 1991, **184**, 1.
28 R. L. Chapman, F. S. Stephens and R. S. Vagg, *Inorg. Chim. Acta*, 1980, **43**, 29; S. T. Mak, V. W. W. Yam, C. M. Che and T. C. W. Mak, *J. Chem. Soc., Dalton Trans.*, 1990, 2555; S. T. Mak, W. T. Wong, V. W. W. Yam, T. F. Lai and C. M. Che, *J. Chem. Soc., Dalton Trans.*, 1991, 1915.
29 M. D. Lind and J. L. Hoard, *Inorg. Chem.*, 1964, **3**, 34.
30 (*a*) T. L. Bohan, *J. Magn. Reson.*, 1977, 109; (*b*) S. Bhattacharya and A. Chakravorty, *Proc. Indian Acad. Sci.*, 1985, **95**, 159; (*c*) P. Basu, S. Bhanja Choudhury, S. Pal and A. Chakravorty, *Inorg. Chem.*, 1989, **28**, 2680; (*d*) D. V. Stynes, H. Noglic and D. W. Thompson, *Inorg. Chem.*, 1991, **30**, 4567; (*e*) D. J. Kennedy, K. S. Murray, P. R. Zwack, H. Homborg and W. Kalz, *Inorg. Chem.*, 1986, **25**, 2539.
31 D. Collison and A. K. Powell, *Inorg. Chem.*, 1990, **29**, 4739; S. C. Tang, S. Koch, G. C. Papaefthymiou, S. Foner, R. B. Frankel, J. A. Ibers and R. H. Holm, *J. Am. Chem. Soc.*, 1976, **98**, 2414; E. T. Kintner and J. H. Dawson, *Inorg. Chem.*, 1991, **30**, 4892; C. A. Reed, T. Mashiko, S. P. Bentley, M. E. Kastner, W. R. Scheidt, K. Spartalian and G. Lang, *J. Am. Chem. Soc.*, 1979, **101**, 2948.
32 X. Tao, D. W. Stephan and P. K. Mascharak, *Inorg. Chem.*, 1987, **26**, 754.

Received 19*th February* 1993; *Paper* 3/01006F